



AUTHOR(S):

TITLE:

YEAR:

Publisher citation:

OpenAIR citation:

Publisher copyright statement:

This is the _____ version of proceedings originally published by _____
and presented at _____
(ISBN _____; eISBN _____; ISSN _____).

OpenAIR takedown statement:

Section 6 of the "Repository policy for OpenAIR @ RGU" (available from <http://www.rgu.ac.uk/staff-and-current-students/library/library-policies/repository-policies>) provides guidance on the criteria under which RGU will consider withdrawing material from OpenAIR. If you believe that this item is subject to any of these criteria, or for any other reason should not be held on OpenAIR, then please contact openair-help@rgu.ac.uk with the details of the item and the nature of your complaint.

This publication is distributed under a CC _____ license.

Computational Fluid Dynamic Analysis of Sand Erosion in 90° Sharp Bend Geometry

M.G Droubi¹*, R. Tebowei¹, S.Z. Islam¹, M. Hossain¹ and E. Mitchell¹

¹School of Engineering, Robert Gordon University, Aberdeen, AB10 7GJ, UK

**corresponding author, E-mail:m.g.droubi@rgu.ac.uk*

Abstract

The prediction of erosion damage due to sand presence during hydrocarbon production is a major threat to the integrity of the production facilities. Sand production from oil and gas reservoirs can cause a significant damage to different pipeline components, and as a consequence, may lead to unwanted maintenance costs and potential environmental damage. In this work, a computational fluid dynamics (CFD) model was developed to investigate how altering flow conditions, pipe geometry and solid particle variables might affect the sand erosion rates at pipe bends. The model was first validated against particle tracks and erosion profiles presented by a published research with reasonable agreement.

Erosion rate was found to decrease as the pipe diameter was increased with significant reductions observed when the pipe diameter was increased by the smallest degree (i.e. from 4" to 6"). Increasing the bend radii of 1.5D, 3D and 5D also resulted in a gradual decrease in maximum erosion rate observed in each test case respectively. However, it was observed that the surface area damaged by erosion increased as the bend radius was increased. It was found also that increasing particle size results in significantly larger erosion rates with different erosion scarring associated with each particle size. Moreover, no direct correlation was observed between increasing the carrier fluid density and the erosion rate. . However, much larger magnitudes of erosion were observed when gas (low density) was the carrier fluid when compared to oil and water individually. Besides, as expected, erosion rate was found to increase significantly with increase in flow velocity.

The final tests conducted were carried out when the distance between two bends in series was increased from 2.5D to 5D and then to 7.5D. Interestingly, erosion was found to increase as the distance between the bends was increased.

Introduction

The prediction of erosion damage caused by solid particles within flow lines is crucial for many industries (e.g. oil and gas). During petroleum production and transportation pipelines, sand particles may be present in hydrocarbon flow from reservoir formation due to increased use of proppants and reservoir fracturing techniques, loss of capillary pressure after water-cut and well ageing [1]. The sand in the flow stream may have a devastating effect and cause major threat to the integrity of the production facilities. Therefore, it is of paramount importance to gain more insights of the nature and severity of pipe erosion in order to precisely predict the erosion rate and identify the pipe locations which are most susceptible to erosion. Pipe bends are most susceptible to damage caused by sand as such components alter the direction in which the production fluid is flowing [2].

Many researchers have used Computational Fluid Dynamics (CFD) to predict pipe erosion rate in different flow conditions and pipe geometries. Edwards *et al.* [2] investigated the effects of erosion in plugged tees and varying bend radius in pipe elbows in order to develop procedures that could be applied within CFD codes for predicting pipe erosion. They claimed that the developed procedure was successful in predicting fluid velocity through the investigated geometries with good agreement in their prediction with results found experimentally for particle penetration rate. McLaury *et al.* [3] developed a model, as an alternative to the API RP 14E, to predict erosion rates in annular flow for cases of horizontal and vertical pipe bend orientation. They found that erosion was greater in magnitude in bends that were vertically orientated. A similar investigation was carried out by Vieira *et al.* [4]. Again, erosion was found to increase significantly in pipe bends that are vertically orientated. It was also found that increasing pipe diameter led to a decrease in erosion rates. Conversely, the addition of a small volume of liquid film into the flow helped to reduce erosion.

The influence of particle size and fluid viscosity on solid particle erosion was investigated by Mansouri *et al.* [5]. However, this investigation was carried out using a submerged jet test with particles impacting on a Coupon, rather than a specific piping geometry. The results were then

compared to those found when the test was replicated using a commercial CFD package. They found that their CFD predictions underestimate the erosion rate. A similar nozzle style test was carried out by Okita *et al* [6], to investigate the influence of particle shape on erosion rate. It was shown that erosion decreased as the carrier fluid viscosity was increased and also that particle shape has a significant effect on the magnitude of erosion. Sharp particles were found to cause higher erosion than in cases where rounded particles were used. It was also shown that CFD predictions showed large variations in predicting erosion ratio when compared to experimental data.

Wang and Shirazi [7] investigated the development of a CFD based correlation that would allow the calculation of penetration rates where the bend radius is varied. The model showed reasonable accuracy when compared with experimental data. It was also concluded that using long radius bends helped to reduce particle erosion in gas flows. Felten [8] investigated the effect of varying the distance between pipe bends in series and the angle between the bends. It was found that beyond a critical point, the distance between double bends has no influence on the erosion rates produced. However, their work was carried out on 1" piping system which is not representative of that found in the oil and gas industry. Barton [9] provided an overview of erosion caused by solid particles in Oil and Gas pipe components, and suggested methods of minimising erosion and reviewed the various models available for predicting erosion. However, each model was found to respond to various test conditions in a different manner and therefore the main conclusion drawn from the analysis was that no one model is suitable for use universally to predict erosion in pipe systems.

Most of the currently available CFD-based erosion models and the experimental data of loop tests focus on the pipe bend with gas–solid flow while few studies have investigated the erosion modelling due to liquid–sand flows. Additionally, it was found in the literature review that very little research has been performed on double-bends (elbows mounted in series). Therefore, in this paper the CFD modelling of erosion caused by solid particles entrained in both gas and liquid, flowing in a 90° sharp bend pipe at different flow conditions is conducted. The effect of different bend geometries, including bend diameter and the distance between double bends were also investigated.

Governing equations

The present study modelled the liquid-sand flow using the Eulerian–Lagrangian multiphase flow modelling method. The liquid is treated as a continuous phase and modelled by solving

the Navier–Stokes conservation equations, while the particles are treated as a discrete phase and solved by tracking a large number of individual solid particles.

The conservation of mass and momentum equations are expressed in Equations (1) and (2).

$$\frac{\partial}{\partial t}(\rho) + \nabla(\rho \vec{v}) = 0 \quad (1)$$

Where:

$$\frac{\partial}{\partial t}(\rho \vec{v}) + \nabla(\rho \vec{v} \vec{v}) = -\nabla p + \nabla(\bar{\tau}) + \rho \vec{g} + \vec{s}_m \quad (2)$$

- S_m – Mass added to continuous phase from dispersed second phase.
- p – Static Pressure
- $\bar{\tau}$ – stress tensor
- $\rho \vec{g}$ – gravitational body force

The stress tensor equation is given by:

Where μ is molecular viscosity and I is the unit tensor

$$\bar{\tau} = \mu \left[(\nabla \vec{v} + \nabla \vec{v}^T) - \frac{2}{3} \nabla \vec{v} I \right] \quad (3)$$

The standard k-ε turbulence model originally developed by Launder and Spalding [10] is used to resolve the flow turbulence. The transport equations for the turbulence kinetic energy, k and the dissipation rate, ε are given by Equations (4) and (5):

$$\frac{\partial}{\partial t}(\rho k) + \frac{\partial}{\partial x_i}(\rho k u_i) = \frac{\partial}{\partial x_j} \left[\left(\mu + \frac{\mu_t}{\sigma_k} \right) \frac{\partial k}{\partial x_j} \right] + G_k + G_b - \rho \varepsilon - Y_M + S_k \quad (4)$$

$$\frac{\partial}{\partial t}(\rho \varepsilon) + \frac{\partial}{\partial x_i}(\rho \varepsilon u_i) = \frac{\partial}{\partial x_j} \left[\left(\mu + \frac{\mu_t}{\sigma_\varepsilon} \right) \frac{\partial \varepsilon}{\partial x_j} \right] + C_{1\varepsilon} \frac{\varepsilon}{k} (G_k + C_{3\varepsilon} G_b) - C_{2\varepsilon} \rho \frac{\varepsilon^2}{k} + S_\varepsilon \quad (5)$$

Where:

- G_k - generation of turbulence kinetic energy due to mean velocity gradients
- G_b - generation of turbulence kinetic energy due to buoyancy
- Y_M - contribution of fluctuating dilation in compressible turbulence to the overall dissipation rate
- σ_k - turbulent Prandtl number for k
- σ_ε - turbulent Prandtl number for ε

- S_k - user defined source term
- S_ε - user defined source term
- $C_{1\varepsilon}, C_{2\varepsilon}, C_{3\varepsilon}$ are constants

The trajectory of each particle is predicted by solving the particle force balance, as expressed

$$\mu_t = \rho C_\mu \frac{k^2}{\varepsilon} \quad (6)$$

in Equation (7).

$$\frac{du_p}{dt} = F_D(\vec{u} - \vec{u}_p) + \frac{\vec{g}(\rho_p - \rho)}{\rho_p} + \vec{F} \quad (7)$$

Where \vec{F} is the acceleration term, $F_D(\vec{u} - \vec{u}_p)$ is drag force per unit particle mass

The drag force is computed using the following relationship

$$F_D = \frac{18\mu}{\rho_p d_p^2} \frac{C_D Re}{24} \quad (8)$$

- \vec{u} - carrier fluid velocity
- \vec{u}_p - particle velocity
- μ - molecular viscosity of fluid
- ρ - fluid density
- ρ_p - particle density
- d_p - particle diameter
- C_D - drag coefficient
- Re - Relative Reynolds number

The relative Reynolds Number, Re , is calculated from the following relationship

$$Re = \frac{\rho d_p |\vec{u} - \vec{u}_p|}{\mu} \quad (9)$$

The drag coefficient, C_D is computed based on Spherical drag law, in which the C_D is given by Equation (10).

$$C_D = a_1 + \frac{a_2}{Re} + \frac{a_3}{Re^2} \quad (10)$$

Where, a_1 , a_2 and a_3 are constants that apply over a wide range of Re given by Morsi and Alexander [11]

Finally, after calculating the flow of liquid and the discrete phase through the model, ANSYS can calculate erosion. The general equation that calculate the rate of erosion [17]:

$$R_{erosion} = \sum_{p=1}^{N \text{ Particles}} \frac{\dot{m}_p C(d_p) f(\alpha) v^{b(v)}}{A_{face}} \quad (11)$$

Where:

- \dot{m}_p - particle mass flow rate
- $C(d_p)$ - function of particle diameter
- α - impact angle of particle path with wall face
- $f(\alpha)$ - function of impact angle
- v - relative particle velocity
- $b(v)$ - function of relative particle velocity
- A_{face} - area of cell face

C , f and b are constant functions, the numerical values of the functions depend on the properties of pipe material. The values specified for the functions C , f and b are 1.8×10^{-9} , 1 and 0, respectively, as recommended by Mazumder [12].

Commented [MH(1)]: I think Majumder values are different.

CFD Model Development

Figure 1 shows the 3-D geometry of the bend pipe generated using ANSYS Design-modeller. The inlet and outlet boundaries of the pipe are shown in the figure. Figure 2 shows the hexahedral mesh structure of the bend pipe geometry. The mesh cells in the pipe wall were generated with 10 inflation layers around the pipe wall, in order to accurately resolve the flow in the pipe near wall.

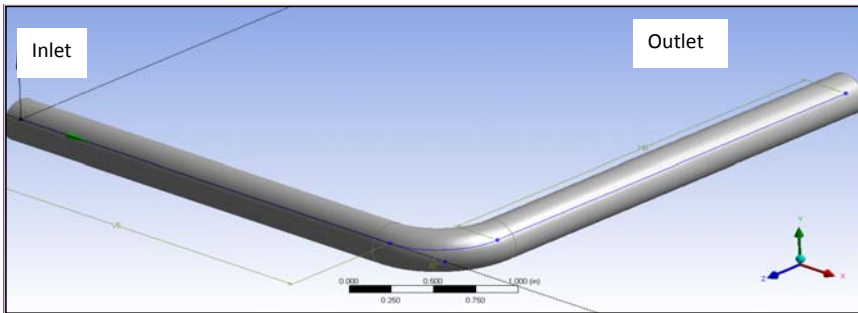


Figure 1: Geometry of the Pipe Model with the Named Sections

Commented [SI (2)]: Dimensions are required

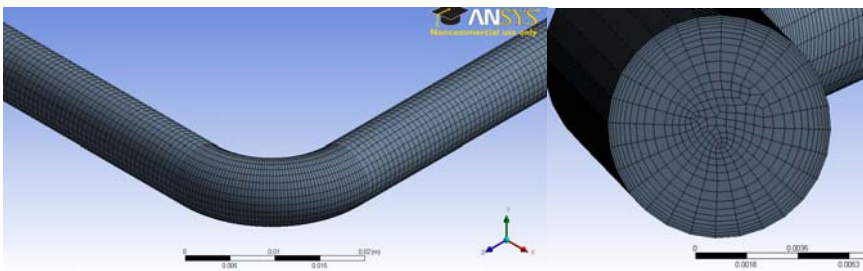


Figure 2: computational mesh used in the simulation

Results

Validation

In order to verify the flow modelling capabilities, a verification study is performed on a 90° elbow. By comparing the predicted erosion rate with the published work of Edwards *et al* [2], the accuracy of the flow solution can be assessed. The shape of the contour plots of erosion shown in Figure 3, shows relatively a good agreement with the maximum erosion occurs in similar locations, at approximately 45 degrees from the pipe inlet. The erosion is also seen to be concentrated on the bend, with minimal erosion occurring downstream of the bend in each case. The similarities in the erosion profiles illustrate that the results collated in the test cases will provide valid qualitative data to analyse erosion. The specific parameters used are shown in Table 1.

Commented [SI (3)]: include

Table 1 - Validation Test Parameters [5]

Parameter	Value
Pipe Diameter	2"
Bend Radius	1.5D
Carrier Fluid Velocity	15.24m/s
Carrier Fluid	Methane Gas
Particle Diameter	150 μ m
Particle Density	2650kg/m ³
Sand Production Rate	4.55kg/day

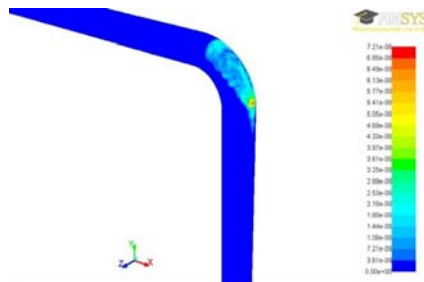


Figure 3: Erosion profiles - Validation

Commented [SI(4)]: Delete the figure

Effect of pipe diameter on erosion rate

Figure 4 shows the effect of pipe diameter on erosion rate for the 4", 6" and 12" test geometries respectively. As can be seen, the surface area affected by erosion increases as the pipe diameter is increased whereas the maximum erosion is reduced. However, the position of the maximum erosion remains approximately constant.

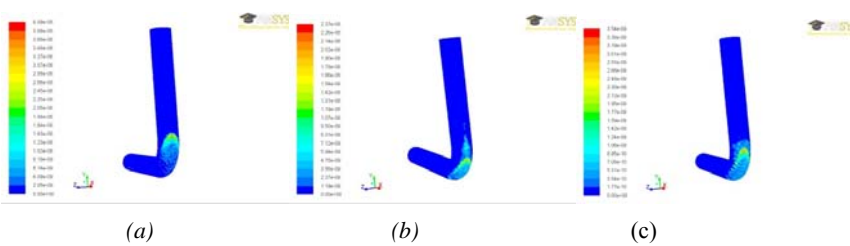


Figure 4: Erosion profiles of pipe bend with different pipe diameter: (a) 4 inches, (b) 6 inches and (c) 12 inches

Figure 5 shows the recorded maximum erosion rate values for each pipe diameter. As can be seen, larger pipe diameter will result in lower maximum erosion rate. Increasing the pipe diameter from 4" to 6" is seen to decrease the maximum erosion occurring by around 42%. However, increasing the pipe diameter from 6" to 12" reduces the maximum erosion rate by 85%. Therefore, using larger diameter piping can increase the life of pipe bends and thus reduce expenditure on maintenance and repair. However, using larger diameter piping will require greater expenditure and greater space on the platform. In some cases it may not be practical to redesign piping networks from 4" or 6" to 12" pipe diameter. However, increasing from 4" to 6" pipe diameter is potentially far more feasible as a method of minimising erosion.

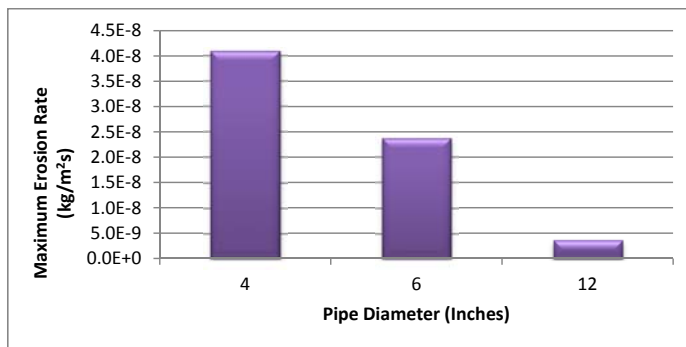


Figure 5: Maximum Erosion Rate vs Pipe Diameter

Effect of bend radius on erosion rate

Figure 6 shows the effect of bend radius on erosion rate for the 1.5D, 3D and 5D test cases respectively. It is clear that altering the pipe bend radius has a significant effect on the magnitude and overall shape of the erosion occurring where the surface area damaged by erosion, downstream of the bend, can be seen to increase as the bend radius is increased from 1.5D to 3D and again from 3D to 5D. However, the location of the maximum erosion in each test case remains in approximately the same location on the bend, as expected from analysing the particle tracks.

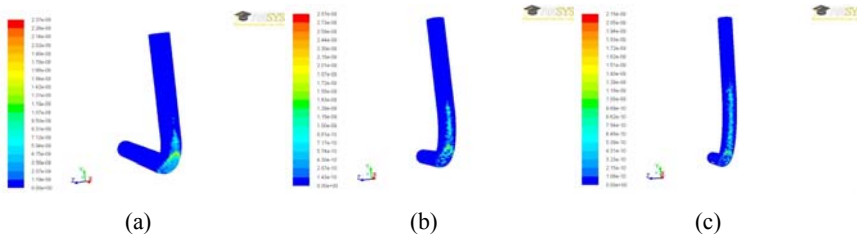


Figure 6: Erosion profiles of pipe bend with different bend radius: (a) 1.5D, (b) 3D and (c) 5D

Figure 7 shows that the maximum erosion rate is reduced as the bend radius is increased which agrees with Wang and Shirazi [7] who found that erosion rates decreased as the bend radius was increased for gas-solid flows. It is observed that doubling the bend radius, from 1.5D to 3D, reduces the maximum erosion by 20% while increasing the bend radius from 3D to 5D resulted in a 24% reduction in erosion. Therefore, increasing the bend radius increases the lifetime of a bend and reducing the frequency of maintenance and replacement work. However, using larger diameter bends will result in increased weight of piping; increased cost to purchase and decreased available space on the platform.

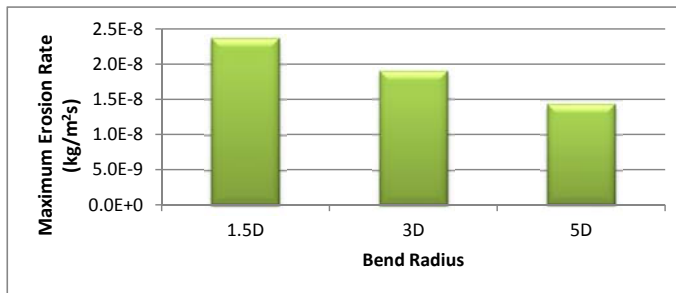


Figure 7: Maximum Erosion Rate vs Bend Radius

Effect of distance between double bends on erosion rate

Figure 10 shows the effect of distance between double bends on erosion rate of the first bend for 2.5D, 5D and 7.5D gaps. The erosion profile appears to be relatively similar in each test case – which is also predicted from the particle tracks. It was observed that the magnitude of erosion in the first bend decreases as the distance between the bends in series is increased. This could be due to the uniformity of the flow from the first bend to the second being extremely turbulent resulting in particles impacting the bend with greater energy and thus resulting in greater erosion. Therefore, it can be seen that increasing the distance upstream of the first bend

results in lower magnitudes of erosion in the first bend, due to the ability of the flow downstream to stabilise.

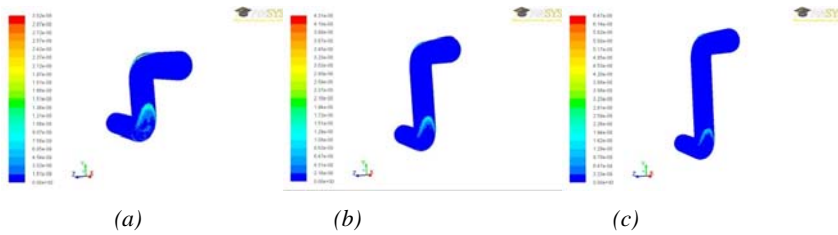


Figure 10: Erosion profiles of the first pipe bend with different distance between bends: (a) 2.5D, (b) 5D and (c) 7.5D

Figures 11 shows the effect of distance between double bends on erosion rate of the second bend. As can be seen, the erosion rate increases as the distance between the bends in series is increased. It is expected that this is largely due to the angle at which the particles impact the second bend.

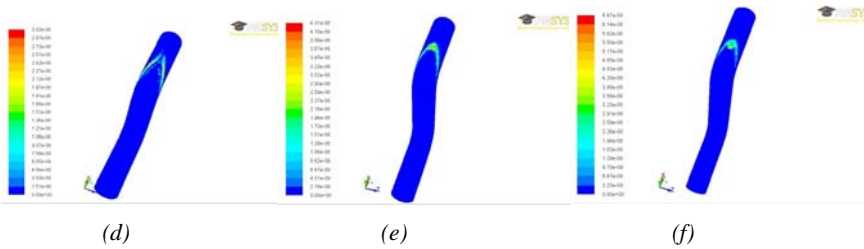


Figure 11: Erosion profiles of the second pipe bend with different distance between bends: (a) 2.5D, (b) 5D and (c) 7.5D

It was observed that the particles in the 2.5D gap impinge the bend normally, and thus, fewer particles impact at the optimum erosion angle of 30° [13]. However, as the distance between the bends is increased, and the particles are more evenly distributed throughout the flow, a greater number of particles impact the bend at the optimum angle and therefore result in greater magnitudes of erosion. This is illustrated in Figures 12 (a) - (c) where the particle velocities in each test case are tracked and coloured in terms of velocity magnitude. Ten tracks were skipped in each case so the results were easier to view.

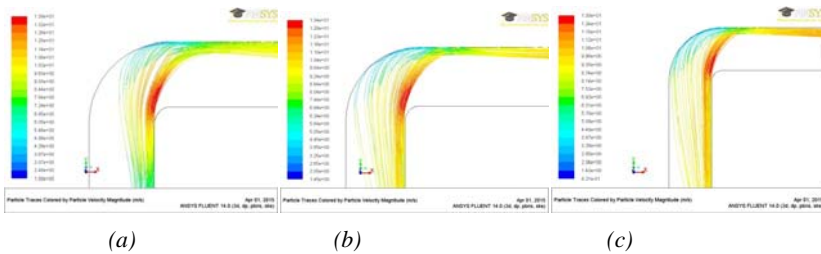


Figure 12: Particle Velocities and trajectories at the second pipe bend with different distance between bends: (a) 2.5D, (b) 5D and(c) 7.5D

Interestingly, Figure 12 (a) shows the highest particle impact velocity at the second bend with the lowest erosion observed. However, Figure 12 (c) shows that the particle trajectories are altered in a manner such that a larger number of particles impact the pipe wall at the optimum impact angle for erosion, and thus higher erosion rates are observed. It is therefore important combine the effect of particle trajectories, and ultimately particle impact angles, in complex pipe geometries. Figure 13 shows that the maximum erosion rate occurring in each test case increases as the distance between bends in series is increased.

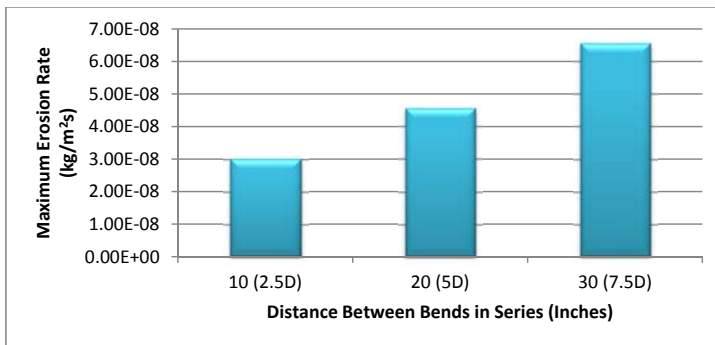


Figure 13: Maximum Erosion Rate at the second bend vs Distance Between Bends in Series

Conclusion

A Eulerian simulation with the k-ε turbulence model was used to simulate the liquid flow in the pipe bend while the Lagrangian particle tracking method was employed for calculating the particle motion. The effects of different parameters on erosion rate were studied with the following conclusion.

The erosion rate increases with carrier fluid velocity and particle diameter increasing, while decreases with bend radius, carrier fluid density and distance between bends in series

increasing. The carrier fluid density has little effect on the change of the erosion rate, particularly, where water was the carrier fluid, when compared to oil. This suggests that in fact there is a direct correlation between the carrier fluid viscosity and the erosion rates calculated, since oil is more viscous than water.

The results in each test case provide qualitative erosion data that illustrate the location of maximum erosion and shape of erosion scarring. Qualitative indications of how varying a number of parameters influence the magnitude of erosion and how often repair and replacement work is required is also provided. However, the erosion magnitudes may differ to those found in real-life applications for a number of reasons. Some of these contributing factors include: insufficient computing power; non-realistic particle injections; and modelling the problem in Steady State instead of Transient.

References

- [1] - Salama M. Sand Production Management. *Journal of Energy Resources Technology*. 2000; 122 (1).
- [2] - Edwards J, McLaury B, Shirazi S. Modeling Solid Particle Erosion in Elbows and Plugged Tees. *Journal of Energy Resources Technology*. 2001; 123 (4).
- [3] - McLaury B, Shirazi S, Viswanathan V, Mazumder , Santos G. Distribution of Sand Particles in Horizontal and Vertical Annular Multiphase Flow in Pipes and the Effects on Sand Erosion. *Journal of Energy Resources Technology*. 2011; 133 (2).
- [4] - Viera R, Kesena N, McLaury B, Shirazi S. Sand Erosion in Multiphase Flow for Low-Liquid Loading and Annular Conditions. *ASME 2012 International Mechanical Engineering Congress and Exposition*. 2012; 7 (1).
- [5] - Mansouri A, Shirazi S, McLaury B. Experimental and Numerical Investigation of the Effect of Viscosity and Particle Size on the Erosion Damage Caused by Solid Particles. *ASME 2014 4th Joint US-European Fluids Engineering Division Summer Meeting*. 2014; 1 (1)
- [6] - Okita R, Zhang Y, McLaury B, Shirazi S, Rybicki E. Effects of Viscosity, Particle Size, and Particle Shape on Erosion in Gas and Liquid Flows.
- [7] - Wang J, Shirazi S. A CFD Based Correlation for Erosion Factor for Long-Radius Elbows and Bends. *Journal of Energy Resources Technology*. 2003; 125 (1)
- [8] - Felten F. Numerical Prediction of Solid Particle Erosion for Elbows Mounted in Series. *Proceedings of the ASME 2014 4th Joint US-European Fluids Engineering Division Summer Meeting*. 2014; 1 (1)

[9] - Barton N. Erosion in Elbow in Hydrocarbon Production Systems: Review Document. *HSE Books*. [serial on the Internet]. 2003 [cited 2014 Oct 01]. Available from: <http://www.hse.gov.uk/research/rrpdf/rr115.pdf>

[10] - Launder, B. E., & Spalding, D. B. (1974). The numerical computation of turbulent flows. *Computer methods in applied mechanics and engineering*, 3(2), 269-289.

[11] Morsi S, Alexander AJ. An investigation of particle trajectories in two-phase flow systems. *Journal of Fluid Mechanics*. 1972 Sep 26;55(02):193-208.

[12] - Mazumder Q. *Tutorial: Investigate Erosion In A 180 Degree U-Bend Using FLUENT*. [homepage on the Internet]. Flint: University of Michigan; [cited 2015 Jan

[13] - Det Norske Veritas. Recommended Practice RP O501 Erosive Wear in Piping Systems. *DNV Recommended Practice*. 2007. (4.2)